Journal of Alloys and Compounds 509 (2011) 5952–5957

Contents lists available at ScienceDirect

Journal of Alloys and Compounds

journal homepage: www.elsevier.com/locate/jallcom

Structural and magnetic properties of the ternary compounds $Gd_2Sc_3X_4$ with X = Si and Ge

E. Gaudin, B. Chevalier*

CNRS, Université de Bordeaux, ICMCB, 87 avenue du Docteur Albert Schweitzer, 33608 Pessac Cedex, France

ARTICLE INFO

Article history:
Received 27 January 2011
Received in revised form 2 March 2011
Accepted 3 March 2011
Available online 10 March 2011

Keywords:
Ternary compounds
X-ray diffraction
Antiferromagnets

ABSTRACT

X-ray diffraction on single crystal performed on $Gd_2Sc_3Si_4$ reveals that this ternary silicide crystallizes as $Gd_2Sc_3Ge_4$ in the orthorhombic $Ce_2Sc_3Si_4$-type with a small deficiency in gadolinium leading to the formula $Gd_{1.88(1)}Sc_3Si_4$. The structure is formed by $[Gd_2Sc_3Si_4]$ slabs with Si–Si interslab covalent bonds. The investigation of the $Gd_2Sc_3Si_4$ and $Gd_2Sc_3Ge_4$ compounds by magnetization, electrical resistivity and specific heat measurements reveals their antiferromagnetic behaviors; $Gd_2Sc_3Si_5$ having a Néel temperature (48–52 K) higher than that observed (22–23 K) for $Gd_2Sc_3Ge_4$.

1. Introduction

The ternary compounds $Gd_2Sc_3Si_4$ and $Gd_2Sc_3Ge_4$ have been prepared and characterized structurally for the first time by Morozkin et al. [1]. Using X-ray powder diffraction, these authors report that these intermetallics adopt the orthorhombic $Ce_2Sc_3Si_4$-type structure [2] an ordered ternary derivative of the Sm_5Ge_4-type (space group *Pnma*) [3]. In $Gd_2Sc_3Si_4$ and $Gd_2Sc_3Ge_4$, Gd atoms occupy one samarium 8*d* site while Sc atoms are distributed on the two other 8*d* and 4*c* sites. More recently, using X-ray diffraction on single crystal, Misra and Miller [4] confirmed that $Gd_2Sc_3Ge_4$ adopts the $Ce_2Sc_3Si_4$-type structure and it was observed a small exchange between gadolinium and scandium on the two 8*d* sites with occupancy ratios Gd:Sc respectively of 0.967:0.033 and 0.031:0.969. Among the compounds adopting the $Ce_2Sc_3Si_4$-type structure, it was reported that $Ce_{1.22}Sc_3Ge_4$ crystallizes with a defect derivative induced by a partial occupancy of the cerium site [5]. These two last studies show that the compounds crystallizing with the orthorhombic $Ce_2Sc_3Si_4$-type structure can exhibit defect or disordered structure. This is why a single-crystal X-ray diffraction investigation of $Gd_2Sc_3Si_4$ was performed and will be presented for the first time in this paper.

It is also interesting to point out that in the series of compounds with structure deriving from the orthorhombic Sm_5Ge_4-type, the existence or not of interslab covalent bonds between germanium or silicon atoms is of importance to understand their crystallographic and physical properties [6,7]. These covalent bonds when they are observed increase the linking between the slabs formed by the rare-earth and the germanium or silicon atoms. For instance it was nicely shown in the Gd_5Si_4–Gd_5Ge_4 system that the making or breaking of these covalent bonds can be compared to the closing or opening of a nano-zipper [6,7].

Concerning, the magnetic properties of these compounds based on Gd, only the temperature dependence between 77 and 300 K of the susceptibility of $Gd_2Sc_3Si_4$ was reported [8]. The ternary silicide exhibits a paramagnetic behavior in this temperature range with a positive (θ_p = 43.6 K) paramagnetic Curie temperature.

Considering that the intermetallics $Gd_2Sc_3Si_4$ and $Gd_2Sc_3Ge_4$ coexist in the Gd–Sc–Si or Ge systems with the ferromagnetic compounds GdScSi and GdScGe showing an unusually high Curie temperatures (T_C = 318 and 320–350 K respectively for GdScSi and GdScGe) [9–11], it is interesting to determine their magnetic properties. In this work, we present and discuss also our results obtained for the first time on the magnetic properties of $Gd_2Sc_3Si_4$ and $Gd_2Sc_3Ge_4$ investigated by electrical resistivity, magnetization and specific heat measurements. These properties are compared to those reported previously on $RE_2Ti_3Ge_4$ (*RE* = Gd, Tb, Dy, Ho and Er) [12] crystallizing as $Gd_2Sc_3Si_4$ and $Gd_2Sc_3Ge_4$ in the orthorhombic $Ce_2Sc_3Si_4$-type.

2. Experimental

Starting materials for the preparation of the $Gd_2Sc_3Si_4$ and $Gd_2Sc_3Ge_4$ samples were ingots of gadolinium (smart-elements), scandium pieces (smart-elements), silicon and germanium pieces (Johnson-Mattey), all with stated purities better than 99.9%. The Gd ingots were then mixed with Sc and Si or Ge pieces in the ideal 2:3:4 atomic ratio and arc-melted under argon (1 atm) purified before with magnesium sponge (673 K). The product buttons were remelted three times to ensure homo-

* Corresponding author. Tel.: +33 5 4000 6336; fax: +33 5 4000 2761.
E-mail address: chevalie@icmcb-bordeaux.cnrs.fr (B. Chevalier).

0925-8388/$ – see front matter © 2011 Elsevier B.V. All rights reserved.
doi:10.1016/j.jallcom.2011.03.023

Table 1
Crystal data and structure refinement[a] for $Gd_{1.88(1)}Sc_3Si_4$ at 293 K.

Chemical formula	$Gd_{1.88(1)}Sc_3Si_4$
Cell setting, space group	Orthorhombic, *Pnma*
a (Å)	7.0728(11)
b (Å)	13.9710(11)
c (Å)	7.379(2)
Z, D_x (Mg m^{-3})	4, 4.943
Radiation type, μ (mm^{-1})	Mo Kα, 20.06
Diffractometer	Nonius Kappa CCD
Absorption correction, shape	Gaussian, triangulare plate
T_{min}, T_{max}	0.734, 0.887
No. of measured, independent reflections, R_{int}	7049, 1307, 0.059
No. of observed reflections ($I > 2\sigma(I)$)	1082
θ_{max} (°)	32.0
Refinement on	F^2
$R[F^2 > 2\sigma(F^2)]$, $wR(F^2)$, S	0.021, 0.050, 1.06
No. of reflections, of refined parameters	1307, 48
Weighting scheme	$w = 1/(\sigma^2(I) + 0.0004I^2)$
$\Delta\rho_{max}$, $\Delta\rho_{min}$ (e Å^{-3})	0.75, −0.92

[a] Computer programs: *Jana2006* [14].

geneity. In the above procedure, the total weight loss (less than 0.2%) was negligible. Annealing was done for one month at 1073 K by enclosing the samples in evacuated quartz tubes. No reaction between the quartz tubes and the samples was observed.

X-ray powder diffraction with the use of a Philips 1050-diffractometer (Cu Kα radiation) was done, before and after annealing, for the phase identification of the samples. The experimental patterns of the annealed samples matched a calculated one [13] indicating pure single phases on the level of X-ray powder diffraction. The orthorhombic parameters obtained through a least-squares routine $a = 7.0700(10)$, $b = 13.9675(13)$ and $c = 7.3757(9)$ Å for $Gd_2Sc_3Si_4$ and $a = 7.2289(9)$, $b = 14.0795(14)$ and $c = 7.4783(8)$ Å for $Gd_2Sc_3Ge_4$ are close to those reported previously [1,4].

The refinement of the crystal structure of $Gd_2Sc_3Si_4$ was performed using single-crystal X-ray diffraction data. The single crystal was isolated from a crushed block of the annealed sample and selected by optical microscopy. Reflection data were collected at room temperature on an Enraf-Nonius Kappa charge coupled device (CCD) area-detector diffractometer using Mo Kα radiation. A Gaussian-type absorption correction was applied, the shape of the single crystal being determined with the video microscope of the diffractometer. Data processing and all refinements were performed with the Jana2006 program package [14]. The structure was refined with the space group *Pnma* (no. 62) and at the end of the refinement the reliability factors R/Rw were equal to 2.10/4.99% with residual electron density in the range [−0.92, +0.75 eÅ^{-3}]. Details of data collections, structure refinements and the atomic parameters are listed respectively in Tables 1 and 2. The interatomic distances are given in Table 3. *Further information on the structure refinements may be obtained from: Fachinformationszentrum Karlsruhe, D-76344 Eggenstein-Leopoldshafen (Germany), by quoting the Registry No's. 422595.*

Magnetization measurements were performed using a Superconducting QUantum Interference Device (SQUID) magnetometer in the temperature range 4.2–300 K and applied fields up to 4.6 T. For electrical resistivity measurements (ρ), a bar of 1.5 mm × 1.5 mm × 5 mm was cut from the annealed buttons. The measurement was carried out above 4.2 K using the standard *dc* four-probe method with silver paint contacts and an intensity current of 10 mA. Because of the presence of microcracks into these bars, the absolute value of ρ could not be determined accurately; for this reason, a normalized representation $\rho(T)/\rho$ (270 K) was given. Heat capacity measurements on the $Gd_2Sc_3Si_4$ and $Gd_2Sc_3Ge_4$ annealed samples were performed by a relaxation method with a Quantum Design PPMS system and using a two-tau model analysis. Data were taken in the 1.8–80 K temperature range. For the latter measurements, the sample was a plate (40–50 mg weight) obtained from the bar used for the electrical resistivity investigation.

3. Results and discussion

During refinement of the structure of $Gd_2Sc_3Ge_4$ [4] a small disorder was observed between gadolinium and scandium atoms on the Gd1 and Sc2 positions (see Table 2 for identifying atoms). In our study devoted to the determination of the crystal structure of $Gd_2Sc_3Si_4$, it appeared that the main deviation from the ideal $Ce_2Sc_3Si_4$-type structure came from the occupancy factor of the Gd1 position. With the ideal model, the reliability factors R/Rw were equal to 2.47/5.92% for 47 parameters. The use of the disordered model of Misra and Miller [4] for $Gd_2Sc_3Ge_4$ led to a decrease of the reliability factors down to 2.08/4.92% for 49 parameters with occupancy of Sc2 position by Gd equal to 0.9(2)% and of Gd1 by Sc equal to 7.39(4)%. It was clear from these results that mixing of gadolinium and scandium on the Sc2 site is not significant whereas an excess of density is clearly evidenced on the Gd1 position. To reduce the electron density on the Gd1 position there are two possibilities that give the same reliability factors for the same number of parameters. With the first model a mixing of gadolinium and scandium is used on the Gd1 position and with the second only a refinement of the occupancy factor of the Gd1 position filled only by gadolinium is made. The calculated formulas are $Gd_{1.828(7)}Sc_{3.172(7)}Si_4$ and $Gd_{1.875(5)}Sc_3Si_4$, respectively. The last model was chosen since it gave a chemical formula closer to the targeting one (Table 2). Moreover, such a defect was previously observed for the homologous compound $Ce_{1.22}Sc_3Ge_4$ [5]. With this final model the reliability factors were equal to 2.10/4.99% for 48 parameters.

In $Gd_2Sc_3Si_4$, the Gd1 and Sc2 atoms form as described for $Gd_2Sc_3Ge_4$ [4] two-dimensional slabs stacked along the *c*-axis (Fig. 1a). In these slabs Sc3 atoms have a pseudo-cubic coordination [4Sc2, 4Gd1] and Si2 and Si3 atoms filled trigonal prismatic voids [4Sc2, 2Gd1] and [2Sc2, 4Gd1], respectively (Fig. 1b). These slabs are in close relationship with the tetragonal U_3Si_2-type structure. On can notice that Sc3 is also in an octahedral site of silicon atoms and the slabs are connected through the Si–Si interslab bonds. A first structural characteristic of this ternary silicide concerns the interatomic distances $d_{Gd1-Gd1}$ between Gd1 atoms (Table 3). Each Gd1 has only four next nearest neighbors at 3.707 (2×), 3.723 and 4.303 Å. This number of neighbors is small in comparison with that observed for the equiatomic compound GdScSi where each Gd atom has eight next nearest neighbors at 3.68 (4×) and 4.234 (4×) Å [15]. A second characteristic is the localization of gadolinium on only one site on contrary to what is observed for the homologous compound $Gd_2Y_3Ge_4$ [16]. This can be attributed to the significant difference in radius between scandium and gadolinium. In $Gd_2Y_3Ge_4$ gadolinium and yttrium atoms, which have almost the same metallic radius, are delocalized over the three *RE* (Rare-Earth) sites. Misra and Miller [16] showed that the *RE3* site (corresponding to the Sc3 position in $Gd_{1.875(5)}Sc_3Si_4$) is of great importance for the magnetic properties. Also in $Gd_2Y_3Ge_4$, a magnetic dilution is obtained through the replacement of gadolinium by yttrium. This may explain why ferromagnetic ordering is still observed for $Gd_2Y_3Ge_4$ and not in $Gd_2Sc_3Si_4$ and $Gd_2Sc_3Ge_4$ (see below). A third interesting point to be discussed is the interslab Si1–Si or Ge1–Ge1 contact (Fig. 1). For $Gd_2Sc_3Ge_4$ [4], this Ge1–Ge1 distance is equal to 2.891 Å (Table 3) and is significantly higher than the sum of two covalent radii (2.40 Å) but significantly lower to the one observed in Gd_5Ge_4 (3.621 Å) [6]. According to the analysis of these interslab distances made by Choe et al. [6,7] a strong covalent character of the Ge1–Ge1 bonding can be expected in $Gd_2Sc_3Ge_4$. For $Gd_{1.88}Sc_3Si_4$

Table 2
Atomic positions and equivalent displacement parameters of $Gd_{1.88(1)}Sc_3Si_4$. The identification of the atoms is similar to that used previously for $Gd_2Sc_3Ge_4$ [4].

Atom	Site	Occupancy	x	y	z	U_{eq} (Å^2)
Gd1	8*d*	0.938(3)	0.00953(2)	0.404016(12)	0.17476(2)	0.00624(6)
Sc2	8*d*	1	0.67061(9)	0.37520(5)	0.82418(8)	0.0056(2)
Sc3	4*c*	1	0.16234(11)	3/4	0.50389(12)	0.0062(2)
Ge1	8*d*	1	0.84184(13)	0.46108(7)	0.53566(13)	0.0076(2)
Ge2	4*c*	1	0.0327(2)	3/4	0.1175(2)	0.0070(3)
Ge3	4*c*	1	0.2870(2)	3/4	0.8729(2)	0.0069(3)

Table 3
Interatomic distances (Å) in $Gd_{1.88(1)}Sc_3Si_4$ and $Gd_2Sc_3Ge_4$ [4].[a]

Gd1-	Si1[b]	2.928[b]	Ge3[c]	2.945[c]	Sc3-	Si2[b]	2.769[b]	Ge2[c]	2.800[c]
	Si3	2.973	Ge1	2.961		Si3	2.806	Ge3	2.864
	Si1	3.023	Ge1	3.110		Si3	2.862	Ge3	2.878
	Si3	3.025	Ge3	3.110		Si1 × 2	2.964	Ge1 × 2	2.961
	Si1	3.037	Ge2	3.148		Si2	2.995	Ge2	2.977
	Si2	3.061	Ge1	3.152		Sc2 × 2	3.212	Sc2 × 2	3.268
	Si1	3.283	Ge1	3.186		Sc2 × 2	3.219	Sc2 × 2	3.283
	Sc3	3.407	Sc3	3.468		Gd1 × 2	3.407	Gd1 × 2	3.468
	Sc3	3.425	Sc3	3.488		Gd1 × 2	3.425	Gd1 × 2	3.488
	Sc2	3.515	Sc2	3.508					
	Sc2	3.550	Sc2	3.576	Si1/Ge1-	Si1	2.543	Sc2	2.742
	Gd1 × 2	3.707	Gd1	3.785		Sc2	2.727	Sc2	2.807
	Gd1	3.723	Gd1 × 2	3.786		Sc2	2.771	Sc2	2.876
						Sc2	2.814	Ge1	2.891
Sc2-	Si1	2.727	Ge1	2.742		Gd1	2.928	Gd1	2.961
	Si2	2.730	Ge2	2.767		Sc3	2.964	Sc3	2.961
	Si2	2.766	Ge2	2.807		Gd1	3.023	Gd1	3.110
	Si1	2.771	Ge1	2.823		Gd1	3.037	Gd1	3.152
	Si1	2.814	Ge1	2.876		Gd1	3.283	Gd1	3.186
	Si3	2.854	Ge3	2.901					
	Sc3	3.212	Sc3	3.268	Si2/Ge2-	Si3	2.548	Ge3	2.757
	Sc3	3.219	Sc3	3.283		Sc2 × 2	2.730	Sc2 × 2	2.767
	Sc2	3.498	Sc2	3.508		Sc2 × 2	2.766	Sc3	2.800
	Gd1	3.515	Gd1	3.552		Sc3	2.769	Sc2 × 2	2.823
	Gd1	3.550	Gd1	3.576		Sc3	2.995	Sc3	2.977
	Sc2 × 2	3.702	Sc2 × 2	2.826		Gd1 × 2	3.061	Gd1 × 2	3.148
					Si3/Ge3-	Si2	2.548	Ge2	2.757
						Sc3	2.806	Sc3	2.864
						Sc2 × 2	2.854	Sc3	2.878
						Sc3	2.862	Sc2 × 2	2.901
						Gd1 × 2	2.973	Gd1 × 2	2.945
						Gd1 × 2	3.025	Gd1 × 2	3.110

[a] Standard deviations are all equal or less than 0.002 Å.
[b] Column corresponding to $Gd_{1.88(1)}Sc_3Si_4$.
[c] Column corresponding to $Gd_2Sc_3Ge_4$.

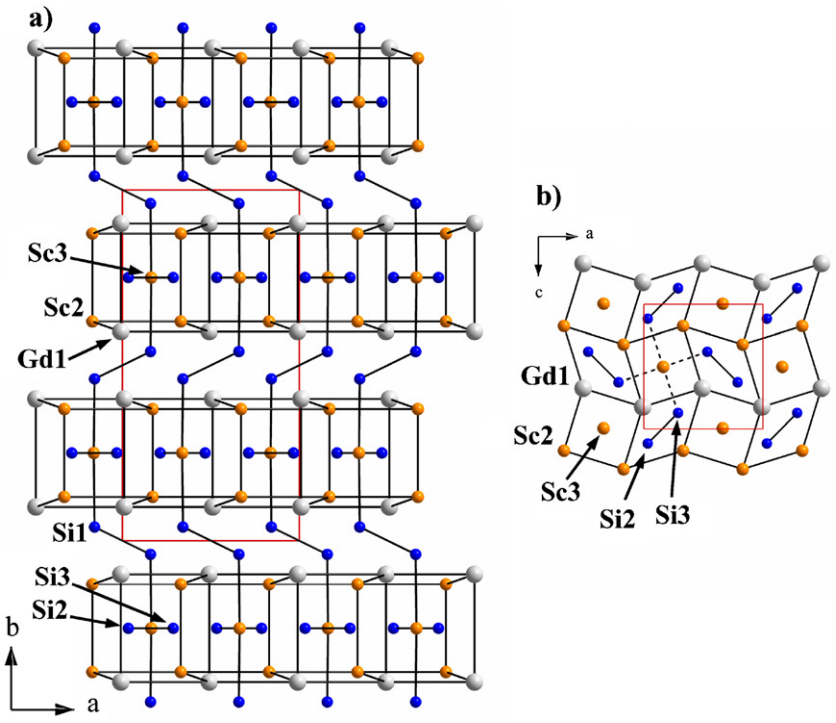

Fig. 1. (a) Projection of the structure of $Gd_2Sc_3Si_4$ along the *c*-axis. (b) View of one U_3Si_2-type slab along the *b*-direction. The Gd–Gd; Gd–Sc bonds corresponding to the cubic and trigonal prism sites filled by Sc3 and Si2–Si3 pairs, respectively, are drawn. The Sc3–Si and Si–Si bonds are also drawn. For (b) only Sc3–Si bonds for one Sc3 atoms are drawn with dashed lines.

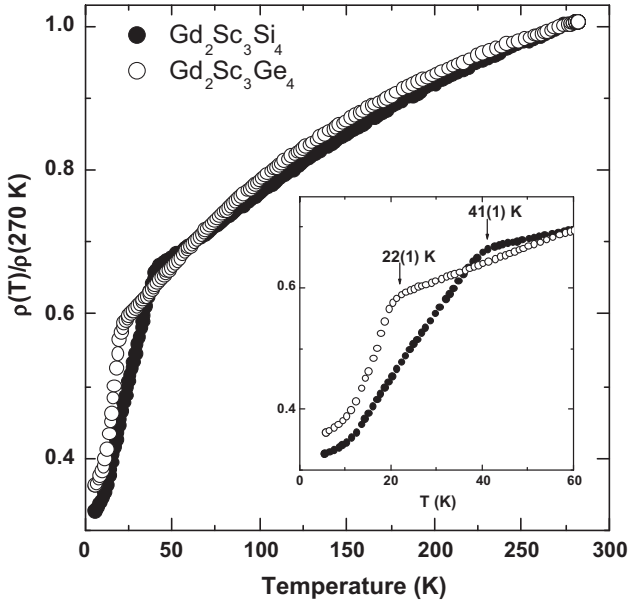

Fig. 2. Temperature dependence of the reduced electrical resistivity $\rho(T)/\rho(270\,K)$ of $Gd_2Sc_3Si_4$ and $Gd_2Sc_3Ge_4$ between 4.2 and 280 K. The inset presents the dependence at low temperatures for $T \leq 60$ K.

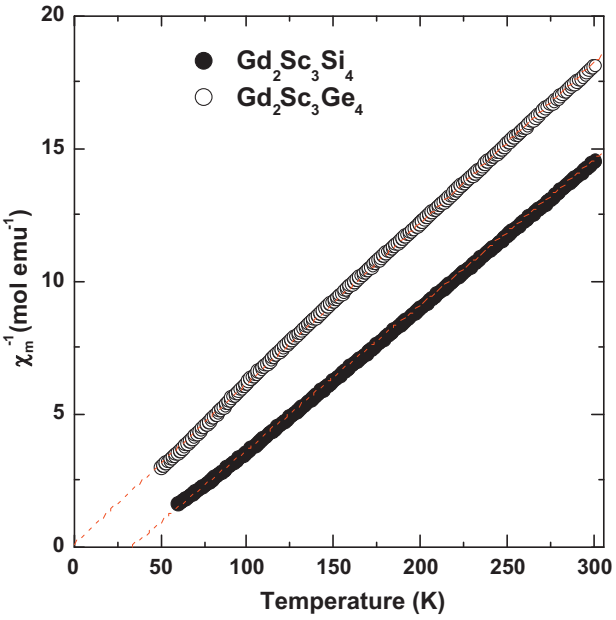

Fig. 3. Temperature dependence, measured for an applied field of 1 T, of the reciprocal magnetic susceptibility χ_m^{-1} for $Gd_2Sc_3Si_4$ and $Gd_2Sc_3Ge_4$. The dashed red lines show the Curie–Weiss law. (For interpretation of the references to color in this figure caption, the reader is referred to the web version of the article.)

the interslab Si1–Si1 distance is equal to 2.543 Å (Table 3) and is similar to the one observed in $Ce_2Sc_3Si_4$ (2.545 Å) [2]. This rather short Si1–Si1 distance is slightly higher than the one observed in Gd_5Si_4 (2.489 Å) [17] and higher of 0.2 Å than the one observed in silicon with diamond-type structure (2.35 Å). From these comparisons, it appears that Si1–Si1 interslab bond in $Gd_{1.88}Sc_3Si_4$ is more covalent than the corresponding Ge1–Ge1 bond in $Gd_2Sc_3Ge_4$. This assumption is also confirmed by the analysis of the *c*/*a* and *b*/*a* unit cell parameters ratios as proposed by Choe et al. [6]. The *b*/*a* and *c*/*a* ratios are equal to 1.98 and 1.04 for $Gd_{1.88}Sc_3Si_4$ and to 1.95 and 1.03 for $Gd_2Sc_3Ge_4$. The higher values of these ratios for the ternary silicide is consistent with a higher covalent Si1–Si1 interslab interaction and the ratios calculated for $Gd_{1.88}Sc_3Si_4$ are exactly in the range of the ones calculated for the compounds adopting the orthorhombic Gd_5Si_4-type structure [6].

The temperature dependence of the reduced electrical resistivity $\rho(T)/\rho(270\,K)$ of $Gd_2Sc_3Si_4$ and $Gd_2Sc_3Ge_4$ is shown in Fig. 2. In the temperature range 280–45 K for $Gd_2Sc_3Si_4$ and 280–25 K for $Gd_2Sc_3Ge_4$, the resistivity exhibits metallic behavior, decreasing almost linearly with the lowering of temperature. A sudden change of slope is detected at 41(1) and 22(1) K, respectively for $Gd_2Sc_3Si_4$ and $Gd_2Sc_3Ge_4$ (inset of Fig. 2) on the curves $\rho(T)/\rho(270\,K)$ *versus* *T*, suggesting the occurrence of a magnetic transition. These last behaviors could be associated with the loss of spin disorder scattering of the conduction electrons appearing at the temperature of this magnetic transition.

The temperature dependence of the reciprocal magnetic susceptibility χ_m^{-1} of $Gd_2Sc_3Si_4$ and $Gd_2Sc_3Ge_4$ measured with a magnetic field of 1 T is shown in Fig. 3. Above 50–60 K, the curves χ_m^{-1} *versus* T are fitted with a Curie–Weiss expression $\chi_m^{-1} = (T-\theta_p)/C_m$ where C_m is the molar Curie constant and θ_p the paramagnetic Curie temperature. The estimated effective moment $\mu_{eff} = (8\,C_m/n)^{1/2}$ (where $n = 2$ is the concentration of Gd^{3+} ions per mol) is found to be around 8.55 and 8.12 μ_B respectively for $Gd_2Sc_3Si_4$ and $Gd_2Sc_3Ge_4$. These μ_{eff} values comparable to that reported previously for $Gd_2Sc_3Si_4$ ($\mu_{eff} = 8.29\mu_B$) [8] are slightly higher than the free-ion moment of the Gd^{3+} ion ($7.94\mu_B$). This suggests a contribution to the magnetic properties of these ternary compounds from the conduction electrons as observed previously for the intermetallic $Gd_4Co_2Mg_3$ [18]. The θ_p values of the $Gd_2Sc_3X_4$ compounds are different: one is positive ($\theta_p = 33$ K for $Gd_2Sc_3Si_4$) and the other slightly negative ($\theta_p = -1.8$ K for $Gd_2Sc_3Ge_4$). The θ_p value observed for $Gd_2Sc_3Si_4$ is close to that reported previously ($\theta_p = 43.6$ K) [8] and indicates the predominance of the ferromagnetic interactions in this ternary silicide. Also, the decrease of the absolute value of θ_p in the sequence $Gd_2Sc_3Si_4 \rightarrow Gd_2Sc_3Ge_4$ suggests that the ternary germanide exhibits a smaller magnetic ordering temperature.

At low temperature, the thermal dependence of the magnetization *M* of $Gd_2Sc_3Si_4$ divided by magnetic field $H = 0.1$ T (Fig. 4) shows the occurrence of a shoulder near $T_N = 49(1)$ K (temperature

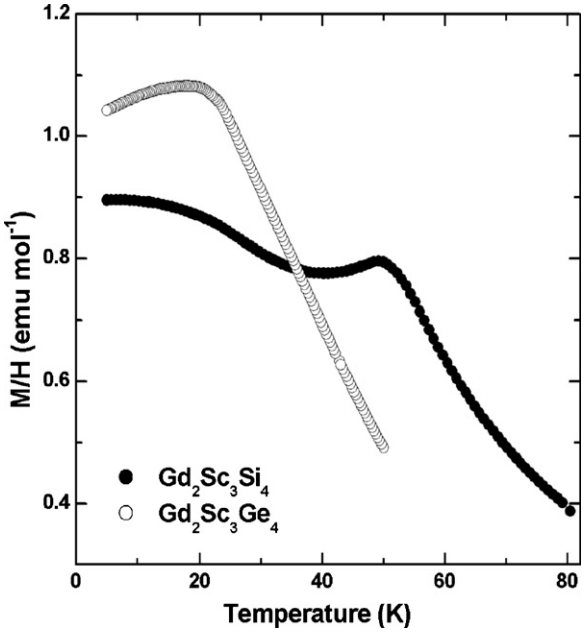

Fig. 4. Temperature dependence of the magnetization *M* of $Gd_2Sc_3Si_4$ and $Gd_2Sc_3Ge_4$ divided by the applied magnetic field of 0.1 T.

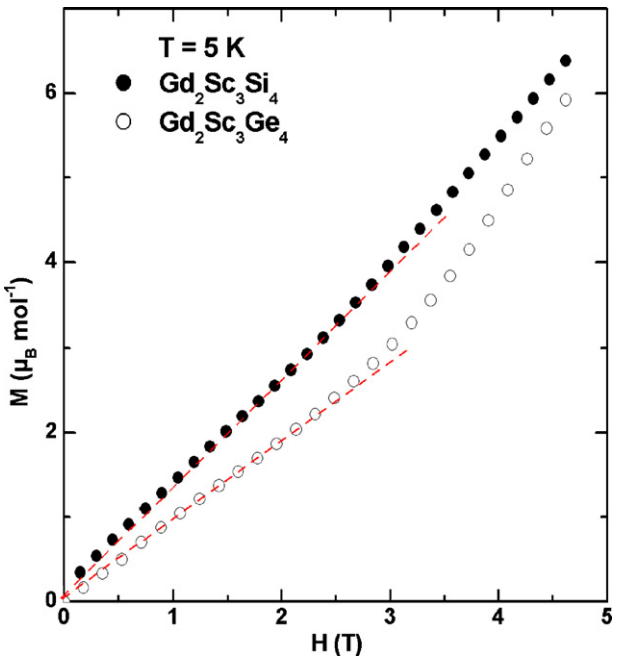

Fig. 5. Field dependence of the magnetization M, at 5 K, for $Gd_2Sc_3Si_4$ and $Gd_2Sc_3Ge_4$.

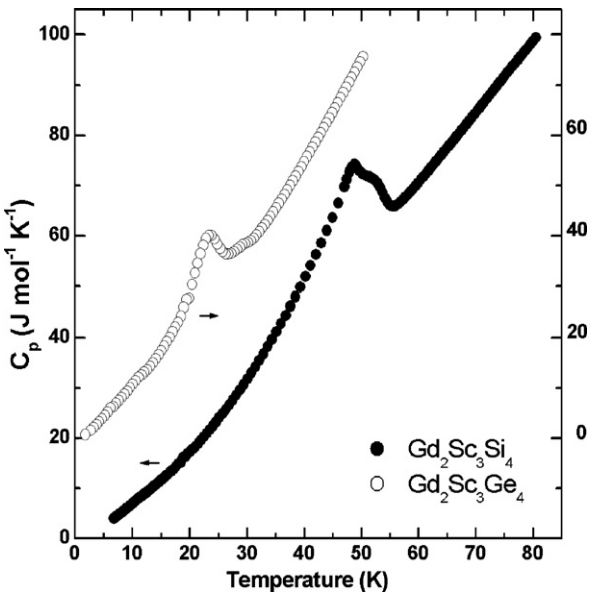

Fig. 6. Temperature dependence of the specific heat C_p for $Gd_2Sc_3Si_4$ and $Gd_2Sc_3Ge_4$. For clarity, the curve concerning $Gd_2Sc_3Ge_4$ was shifted vertically.

defined as the maximum of the shoulder). This behavior suggests that the ternary silicide orders antiferromagnetically at this last temperature. Below T_N, the curve M/H *versus* T presents an increase of the magnetization, owing to undetected impurities or a modification of the magnetic ordering induced by the applied field H as observed for a metamagnetic transition. This Néel temperature $T_N = 49(1)$ K determined by magnetization measurements is higher than that where the electrical resistivity presents a sudden decrease (Fig. 2). The curve M/H *versus* T for $Gd_2Sc_3Ge_4$ passes through a broad maximum around $T_N = 22(2)$ K when the temperature decreases as for an antiferromagnet but the decrease of the magnetization below T_N is very weak. In this case, the T_N temperature is in agreement with that where a decrease of the electrical resistivity is observed (Fig. 2). The decrease of the T_N temperature in the sequence $Gd_2Sc_3Si_4 \rightarrow Gd_2Sc_3Ge_4$ is in accordance with the diminution of the absolute value of θ_p reported above. Also, this decrease of T_N when Si is replaced by Ge can be explained considering the two parameters governing the indirect RKKY magnetic interactions: (i) the interatomic distances Gd1–Gd1 are smaller in the ternary silicide $Gd_2Sc_3Si_4$ (Table 3) and (ii) the structural determination of the two compounds indicates that the Si1–Si1 interslab bond is more covalent than the Ge1–Ge1 interslab bond (Table 3) suggesting a difference between the electronic structures of these intermetallics; for instance the density of states at the Fermi level. The determination of the electronic structures is planned using DFT band structure calculations.

The antiferromagnetic ordering of $Gd_2Sc_3Si_4$ and $Gd_2Sc_3Ge_4$ is further corroborated by the field-dependent behavior of their magnetizations measured at 5 K (Fig. 5). At this temperature, in the antiferromagnetic range, M of $Gd_2Sc_3Si_4$ and $Gd_2Sc_3Ge_4$ increases almost linearly at low magnetic fields and more rapidly above 2.8(2) and 2.5(2) T, respectively. This behavior reveals the appearance of a magnetic transition induced by the applied magnetic field as observed in many antiferromagnets (spin-flip or spin-flop transition) [18].

Specific heat C_p measurements provide further support to the occurrence of an antiferromagnetic ordering for $Gd_2Sc_3Si_4$ and $Gd_2Sc_3Ge_4$. As shown in Fig. 6, presenting the curves C_p *versus* T for these compounds, the most important feature is the well-defined λ-type anomaly signaling the magnetic transition of $Gd_2Sc_3Ge_4$. For this ternary germanide, the T_N ordering temperature associated with the maximum at 23(1) K, is in excellent agreement with that determined from magnetization and electrical resistivity measurements. On the contrary, the curve C_p *versus* T determined for $Gd_2Sc_3Si_4$ exhibits a shoulder near 52(1) K and a peak around 48(1) K; this behavior suggests the existence in a short temperature range of two magnetic transitions for the ternary silicide. The temperature where the maximum of the curve C_p *versus* T is observed agrees with that determined by magnetization measurements.

In conclusion, $Gd_2Sc_3Si_4$ (or $Gd_{1.88}Sc_3Si_4$) and $Gd_2Sc_3Ge_4$ adopt the orthorhombic $Ce_2Sc_3Si_4$-type; the structure of $Gd_2Sc_3Si_4$ was determined for the first time using X-ray diffraction on single crystal. These two compounds are found to have antiferromagnetic ground state having some unusual features: (i) a double magnetic transition evidenced around 52–48 K for $Gd_2Sc_3Si_5$ by specific heat measurement and (ii) the absence below $T_N = 22(2)$ K of a clear decrease of the magnetization of $Gd_2Sc_3Ge_4$. But the Néel temperature of the ternary silicide is higher than that observed for the ternary germanide. The magnetic properties of $Gd_2Sc_3Si_4$ and $Gd_2Sc_3Ge_4$ are comparable to those reported previously on the antiferromagnets $RE_2Ti_3Ge_4$ (RE = Tb, Dy, Ho) [12] but different to those observed for the ferromagnet $Gd_2Ti_3Ge_4$. But it is important to say that for instance in the sequence $Gd_2Ti_3Ge_4 \rightarrow Gd_2Sc_3Ge_4$, the unit cell volume increases strongly (+11.5%) which have an influence on the indirect RKKY interactions governing the magnetic properties of the intermetallics.

Acknowledgement

The authors thank R. Decourt for his assistance during the specific heat measurements.

References

[1] A.V. Morozkin, Y.D. Seropegin, V.K. Portnoy, A.V. Leonov, I.A. Sviridov, J. Alloys Compd. 281 (1998) L1–L2.
[2] I.R. Mokraya, O.I. Bodak, E.I. Gladyshevskii, Kristallografiya 24 (1979) 729–730.
[3] G.S. Smith, Q. Johnson, A.G. Tharp, Acta Crystallogr. 22 (1967) 269–272.
[4] S. Misra, G.J. Miller, Acta Crystallogr. E65 (2009), i25.
[5] Z.M. Shpyrka, V.A. Bruskov, I.R. Mokraya, V.K. Pecharskii, O.I. Bodak, P.Y. Zavalii, Izvestiya Akademii Nauk SSSR Neorganicheskie Materialy 26 (1990) 969–972.

[6] W. Choe, A.O. Pecharsky, M. Worle, G.J. Miller, Inorg. Chem. 42 (2003) 8223–8229.
[7] W. Choe, G.J. Miller, J. Meyers, S. Chumbley, A.O. Pecharsky, Chem. Mater. 15 (2003) 1413–1419.
[8] S.A. Nikitin, A.E. Bogdanov, A.V. Morozkin, Phys. Solid State 41 (1999) 1656–1657.
[9] S.A. Nikitin, I.A. Ovtchenkova, Y.V. Skourski, A.V. Morozkin, J. Alloys Compd. 345 (2002) 50–53.
[10] P. Manfrinetti, M. Pani, A. Palenzona, S.K. Dhar, S. Singh, J. Alloys Compd. 334 (2002) 9–13.
[11] S.N. Mishra, J. Phys.: Condens. Matter 21 (2009) 115601 (11pp).
[12] R. Nirmala, V. Sankaranarayanan, K. Sethupathi, G. Rangarajan, A.V. Morozkin, D.C. Kundaliya, S.K. Malik, J. Appl. Phys. 95 (2004) 7079–7081.
[13] K. Yvon, W. Jeitschko, E. Parthé, J. Appl. Crystallogr. 10 (1977) 73–74.
[14] V. Petricek, M. Dusek, L. Palatinus, Jana2006. The Crystallographic Computing System, Institute of Physics, Praha, Czech Republic, 2006.
[15] A.V. Morozkin, Y.D. Seropegin, V.K. Portnoy, A.V. Leonov, I.A. Sviridov, J. Alloys Compd. 278 (1998) L1–L5.
[16] S. Misra, G.J. Miller, J. Am. Chem. Soc. 130 (2008) 13900–13911.
[17] S. Misra, G.J. Miller, J. Solid State Chem. 179 (2006) 2290–2297.
[18] S. Gorsse, B. Chevalier, S. Tuncel, R. Pöttgen, J. Solid State Chem. 182 (2009) 949–953.